Journal of Advances in Mathematics and Computer Science

36(4): 62-78, 2021; Article no.JAMCS.68717
ISSN: 2456-9968
(Past name: British Journal of Mathematics & Computer Science, Past ISSN: 2231-0851)

A Polygonal Finite Element Method for Stokes Equations

Xinjiang Chen[1*]

[1]School of Mathematical Sciences, Nanjing Normal University 1 Wenyuan Rd., Qixia District, Nanjing, 210023 China.

Author's contribution

The sole author designed, analysed, interpreted and prepared the manuscript.

Article Information

DOI: 10.9734/JAMCS/2021/v36i430357
Editor(s):
(1) Dr. Francisco Welington de Sousa Lima, Universidade Federal do Piauí, Brazil.
Reviewers:
(1) Lim Eng Aik, Universiti Malaysia Perlis, Malaysia.
(2) Paula Cristiane Pinto Mesquita Pardal , USP (University of São Paulo), Brazil.
Complete Peer review History: http://www.sdiarticle4.com/review-history/68717

Original Research Article

Received 10 March 2021
Accepted 13 May 2021
Published 14 May 2021

Abstract

In this paper, we extend the Bernardi-Raugel element [1] to convex polygonal meshes by using the generalized barycentric coordinates. Comparing to traditional discretizations defined on triangular and rectangular meshes, polygonal meshes can be more flexible when dealing with complicated domains or domains with curved boundaries. Theoretical analysis of the new element follows the standard mixed finite element theory for Stokes equations, i.e., we shall prove the discrete inf-sup condition (LBB condition) by constructing a Fortin operator. Because there is no scaling argument on polygonal meshes and the generalized barycentric coordinates are in general not polynomials, special treatments are required in the analysis. We prove that the extended Bernardi-Raugel element has optimal convergence rates. Supporting numerical results are also presented.

Keywords: Mixed finite element method; stokes equations; generalized barycentric coordinates.

1 Introduction

Let $\Omega \subset \mathbb{R}^2$ be a polygon. We consider the following Stokes equation:

**Corresponding author: Email: chenxinjiang94@163.com;*

$$\begin{cases} -\Delta u + \nabla p = f & in\ \Omega, \\ div\ u = 0 & in\ \Omega, \\ u = 0 & on\ \partial\Omega, \end{cases} \tag{1.1}$$

where u is the velocity, p is the pressure, and f is the given body force.

When discretizing Equation (1.1) using the finite element method, the discrete spaces for the velocity and the pressure need to be stable, i.e., satisfying the discrete inf-sup (LBB) condition, in order for the method to converge. Readers may refer to the books [2,3] and references therein for the numerous works in this area. On two dimensional triangular/quadrilateral meshes, the discretization using continuous piecewise linears/bilinears for the velocity and piecewise constants for the pressure, which we will call the PIPO/QIPO element, does not satisfy the LBB condition. However, researchers have long being aware that the actual performance of the PIPO/QIPO element is mesh dependent. The PIPO element does not converge at all on most meshes except for the criss-cross ones (see Example 8.10.2 in [4]), on which it behaves similarly to a QIPO elemen- t defined on the underlying quadrilaterals. The QIPO element is equally complicated. Using a macro-element technique [5], on regular quadrilateral meshes one can prove that the QIPO element gives optimal approximation for the velocity, while the pressure often admits the so-called "spurious modes" [6,7]. Moreover, numerical experiments have shown that on general distort- ed quadrilateral meshes, the spurious pressure mode may disappear. So far there is no theoretical explanation for this yet (see Section 8.10.2 in [4]). But from the numerical point of view, such a phenomenon intrigues a question on how a similar discretization would behave on regular and irregular polygonal meshes. And if is not sable, is it possible to make it stable by the well-known technique of adding bubbles to the velocity space?

In the last decade, polygonal/polyhedral meshes have gained considerable attention in the scientific computing community partly due to their flexibility when dealing with complicated domains or domains with curved boundaries. By using the generalized barycentric coordinates (GBC- s) [8, 9, 10, 11, 12], researchers have extended the $P1/Q1$ conforming finite element to general polygonal meshes [13,14,15]. Based on these, it is indeed straight-forward to extend the PIPO/QIPO element to polygonal meshes.

In [16], Talischi et al. investigated a direct extension of the PIPO/QIPO element to polygonal meshes. Following an argument given in [17] for the mimetic finite difference method, they get a sufficient condition for the discretization to be stable: that is, if every internal vertex in the mesh is connected to at most three edges. The stability is not clear on meshes that do not satisfy this condition, and it certainly fails on most triangular and quadrilateral ones. Later, in [18] Vu-Huu et al. considered an extension of the PIPI element, where both the velocity and the pressure are discretized by continuous piecewise GBCs. Since one would not expect the PIPI element to be stable in general, a stabilization term based on the polynomial pressure projection [19] is added to ensure the convergence of the discretization. The same authors of [18] also considered an extension of the MINI element in [20], which is essentially the extended PIPI element with element-wise bubbles added to the velocity space. Unfortunately, although the MINI element is stable on triangular meshes, numerical calculation has shown that the extended MINI element (with its particular choice of bubbles) is not stable in general. Again, a stabilization is required to ensure the convergence of the discretization.

We notice that previous extensions given in [16, 20, 18] require either special meshes or stabilizations in order to converge. The aim of this paper is to construct a stable finite element discretization for the Stokes equation (1.1) on arbitrary polygonal meshes, by simply adding bubbles to the velocity space of the extended PIPO/QIPO element. To this end, we borrow the idea from the Bernardi-Raugel (BR) element [1]. On triangular and quadrilateral meshes, the BR element is essentially the PIPO/QIQO element with edge bubbles added to the velocity space. We extend this element to polygonal meshes using GBCs. We shall prove that the extension satisfies the LBB condition on arbitrary convex polygonal meshes and thus provides optimal approximation to both the velocity and the pressure. The analysis follows the standard one for the triangular/quadrilateral BR element, but requires many modifications because there is no scaling argument on polygonal meshes and the generalized barycentric coordinates are in general not polynomials.

The paper is organized as follows. In Section 2, we present the definition of GBCs and construct a Clément interpolation associated with the GBCs. We also prove the stability and approximation property of the Clément interpolation. In Section 3, the extended BR element is defined, with its well-posedness and approximation properties analyzed. Finally, in Section 4, supporting numerical results are presented.

2 Generalized Barycentric Coordinates and the Clément Interpolation

In this section, we briefly introduce the generalized barycentric coordinates [8, 9, 10, 11, 12], and then define a Clément type interpolation [21] associated with the GBC.

Let $T \subset \mathbb{R}^2$ be a polygon with vertices v_i, $1 \le i \le n$, ordered counter-clockwise. We use modular arithmetic to extend the index i beyond the range of $\{1, ..., n\}$, for example, setting $v_0 = v_n$, $v_{n+1} = v_1$, etc. Functions λ_i, for $i = 1, ..., n$, are called the a set of GBCs on T, if they satisfy

(1) (Non-negativity) All λ_i, for $1 \le i \le n$, have non-negative value on T;
(2) (Linear precision) For any linear function $L(x)$ defined on T, one has

$$L(x) = \sum_{i=1}^{n} L(v_i)\lambda_i(x) \text{ , for all } x \in T.$$

The linear precision property is equivalent to the combination of the unit decomposition and the Lagrange properties [9]:

$$\sum_{i=1}^{n} \lambda_i = 1, \sum_{i=1}^{n} \lambda_i v_i = x. \tag{2.1}$$

It is clear that $span\{\lambda_i, 1 \le i \le n\}$ contains the space of all linear polynomials.

When $n = 3$, there is a unique GBC that is the traditional barycentric coordinates. When $n \ge 4$, there are more than one GBCs. As an example, we present the formula for the Wachspress GBC [11], which is defined only on convex polygons. Denote by e_i the edge of T pointing from v_i to v_{i+1}, and by n_i the unit outward normal vector on the edge e_i. For a point $x \in T$, denote by $h(x)$ the distance from x to the edge e_i, i.e., $h_i(x) = (v_i - x) \cdot n_i$. Then a formula for computing the Wachspress GBCs, given by Meyers et al. [22], is

$$\lambda_i(x) = \frac{w_i(x)}{W(x)}, \tag{2.2}$$

where

$$w_i(x) = \det\left[\frac{n_{i-1}}{h_{i-1}(x)}, \frac{n_i}{h_i(x)}\right] \text{ and } W = \sum_{i=1}^{n} w_i.$$

When T is a triangle, the Wachspress GBC is identical to the traditional barycentric coordinates. On general polygons, it consists of rational functions by definition.

By definition, the value of λ_i on the jth vertex of T is δ_{ij}, and the restriction of λ_i on an edge of T is linear. This makes GBCs suitable for constructing H^1 conforming finite element spaces. To this end, we first introduce the standard notation of Sobolev spaces. On a given set $T \subset \mathbb{R}^2$, denote by $H^s(T)$ the usual Sobolev space equipped with the norm $\| \cdot \|_{s,T}$ and the semi-norm $| \cdot |_{s,T}$. When $s = 0$, $H^0(T)$ coincides with the square integrable space $L^2(T)$ and we simply denote the L^2 norm on T by $\| \ \|_T$. Denote by $)_T$ and $<\cdot, \cdot> T$ the L^2 inner-product and the duality form, respectively, in T. When $T = \Omega$, we suppress the subscript T in the norm and the inner-product, for example, $\| \cdot \|_s = \| \cdot \|_{s,\Omega}$, $\| \cdot \| = \| \cdot \|_{\Omega}$, and $(\cdot\ ,\ \cdot) = (\cdot\ ,\ \cdot)_{\Omega}$. Denote by $H_0^s(\Omega)$ the closure of $C_0^{\infty}(\Omega)$ in H^s for $s \ge 0$, and by L_0^2 () the mean value free subspace of L^2. Finally, all the above-defined notations can be easily extended to vector and tensor spaces, using the usual tensor products.

Let $\mathcal{T}_h$ be a polygonal mesh on the domain Ω. For simplicity, we assume that all polygons in $\mathcal{T}_h$ are convex. For each $T \in \mathcal{T}_h$, denote by h_T the diameter of T, by ρ_T the diameter of the largest disk in T such that T is star-shaped with respect to, and by $h_{*,T}$ the minimum distance between a vertex of T and a non-incidental edge, i.e., $h_{*,T} := \min_{i=1,...,n} \left(\min_{j \ne i-1,i} h_j(v_i) \right)$. We assume that $\mathcal{T}_h$ satisfies the following regularity assumptions:

(H1) There exists a constant $C > 0$ such that $h_T \le C\rho_T$ for all $T \in \mathcal{T}_h$;

(H2) There exists a constant $C > 0$ such that $h_{*,T} \geq Ch_T$ for all $T \in \mathcal{T}_h$;

(H3) The number of vertices of each polygon in $\mathcal{T}_h$ is uniformly bounded above.

(H4) $\mathcal{T}_h$ is quasi-uniform with the characteristic size $h \triangleq \max_{T\in\mathcal{T}_h} h_T$, i.e., there exists a constant $C > 0$ such that $h_T \geq Ch$ for all $T \in \mathcal{T}_h$.

Remark 2.1. *Assumption* $(H2)$ *immediately implies that each edge of the mesh* $\mathcal{T}_h$ *has length greater than or equal to* Ch_T. *When* T *is convex, assumption* $(H2)$ *also implies assumption* $(H3)$. *Here we list them separately to facilitate later discussions*.

Since $\mathcal{T}_h$ is quasi-uniform, we will use h instead of h_T in the rest of the paper. On a convex polygon T, assumption (H1) immediately implies the bramble-Hilbert lemma [2]

$$inf|v - \chi|_{k,T} \leq Ch^{q-k}|v|_{q,T}, \text{ for } 0 \leq k \leq q \text{ and } v \in H^q(T), T \in \mathcal{T}_h \quad (2.3)$$
$$\chi \in P_k(T)$$

and by [23], conditions (H1) and (H3) imply the following trace inequality

$$\|v\|^2_{\partial T} \leq C(h^{-1}\|v\|^2_T + h\|\nabla v\|^2_T) \text{ , for all } v \in H^1(T) \text{ ,} \quad (2.4)$$

where the general constant C in both (2.3) and (2.4) is independent of h or the shape of T.

The GBCs have bounds $0 \leq \lambda_i(x) \leq 1$ for all $x \in T$. Moreover, a gradient bound has been proved in [24,25,26] for Wachspress, Sibson, and mean value coordinates. This bound is essential to the finite element analysis to be given later.

Lemma 2.1. *On a convex polygon* T *satisying assumptions* $(Hl) - (H4)$, *the Wachspress, Sibson, and mean value coordinates satisy*

$$\sup_{\boldsymbol{x}\in T} \sum_{i=1}^{n} |\nabla \lambda_i(\boldsymbol{x})| \leq Ch^{-1},$$

where C *is a constant independent of* h *or the shape of* T.

Proof. The proof for the Wachspress coordinates can be found in [24], with the right-hand side of the inequality being $4/h_{*,T}$. For the Sibson and mean value coordinates, their gradient bounds follow from a simple uniform scaling of Lemma 7 in [25] and Theorem 1 in [26], respectively. Although the mean value coordinates can be defined on nonconvex polygons, but the proof in [26] is only for convex polygons.

The gradient bounds for the Sibson and mean value coordinates hold even if (H2) is replaced by a weaker assumption that all edges of the polygon have length greater than Ch. □

Then, we define an H^1 conforming finite element space on $\mathcal{T}_h$ as follows:

$$\Lambda_h = \{ v \in C^0(\Omega) \text{ such that } v|\tau \in \Lambda_T \text{ for all } T \in \mathcal{T}_h\} \subset H^1(\Omega)$$

where $\Lambda_T = span\{\lambda_i, 1 \leq i \leq n\}$ is spanned by the GBCs on T. It is clear that a function in Λ_h is uniquely determined by its values at all vertices of $\mathcal{T}_h$. Similarly, one can define a subspace of H_0^1 (Ω) as follows:

$$\Lambda_{0,h} = \{ v \in \Lambda_h \text{ such that } v|_{\partial\Omega} = 0\}.$$

It is well known that a nodal value interpolation into Λ_h or $\Lambda_{0,h}$ requires $H^s(\Omega)$ functions, with $s > 1$. It can not be defined on H^1 A popular substitution is the Clément interpolation [21, 27]. The Clément interpolation has

been well-studied on triangular and rectangular meshes. But we have not found any related work for GBCs defined on polygonal meshes. Given that the GBCs are no longer polynomials and the scaling argument does not work on polygons, it is necessary to carefully examine the definition and the approximation error of the Clément interpolation for GBCs. The details are given in the rest of this section, which basically follows the analysis in the original paper by Clément [21] but with some modifications to adapt to the GBC case.

Denote by $\mathcal{V}_h$ the set of all vertices in $\mathcal{T}_h$, and N the cardinality of $\mathcal{V}_h$. Without loss of generality, we assume that the first N_0 vertices lie in the interior of Ω and the rest lie on $\partial\Omega$. Let $\{\varphi_i\}_{i=1}^N$ be a set of basis for Λ_h satisfying $\varphi_i(v_j) = \delta_{ij}$ for $j = 1, ..., n$. Let

$$S_i = \overline{supp\varphi_i \cap \Omega},$$

and denote by $P_k(S_i)$ the space of all polynomials with degree no more than k on S_i. Let $Q_i : H^1(S_i) \to P_1(S_i)$ be the L^2 orthogonal projection. Define the Clément interpolations $\Pi : H^1(\Omega) \to \Lambda_h$ and $\Pi_0 : H_0^1(\Omega) \to \Lambda_{0,h}$ as follows:

$$\Pi v = \sum_{i=1}^N Q_i\, v(v_i)\varphi_i \text{ and } \Pi_0 v = \sum_{i=1}^{N_0} Q_i\, v(v_i)\varphi_i. \tag{2.5}$$

In order to carry out the interpolation error analysis for Π and Π_0, we make two additional assumptions on the mesh:

(H5) Each S_i intersects with only a finite number of polygons in $\mathcal{T}_h$.

(H6) Each S_i contains a disk centered at v_i with radius r_i, is star-shaped with respect to the disk, and there exists a constant $C > 0$ such that $h \le Cr_i$ for all S_i.

Then by [2], the Bramble-Hilbert lemma holds on S_i, that is

$$\inf_{\chi \in P_k(S_i)} |v - \chi|_{k,S_i} \le Ch^{q-k}|v|_{q,S_i}, \qquad \text{for } 0 \le k \le q \text{ and } v \in H^q(S_i), \tag{2.6}$$

where the constant C depends on the ratio h/r_i but not on the shape of S_i.

Now, we can prove the following H^1 stability of the local L^2 projection:

Lemma 2.2. *Under the condition* $(H6)$, *one has*

$|Q_i v|_{1,S_i} \le C|v|_{1,S_i}$, for all $v \in H^1(S_i)$,

where the constant C *is independent of* S_i.

Proof. This result is known on triangular meshes, for example, see Lemma 3.3 in [28]. However, the proof needs to be modified on $polygonal \wedge$ meshes since the standard scaling argument no longer works. We define a reference polygon $\hat{S}_i$ through magnifying S_i by a factor of $\frac{1}{h}$. Then, condition (H6) ensures that $\hat{S}_i$ lie between two concentric disks, an inner disk B_0 with radius $\frac{r_i}{h} = O(1)$ and an outer disk B_1 with radius $\frac{\max_{T \in S_i} h_T}{h} = O(1)$. Denote by V the value of function v on $\hat{S}_i$, and $\hat{Q}_i$ the L^2-projection onto $P_1(\hat{S}_i)$. A simple calculation shows that

$$|\hat{Q}_i\hat{v}|_{1,\hat{S}_i} \le |\hat{Q}_i\hat{v}|_{1,B_1} \le C\|\hat{Q}_i\hat{v}\|_{B_0} \le C\|\hat{Q}_i\hat{v}\|_{\hat{S}_i} \le \|\hat{v}\|_{\hat{S}_i} \le \|\hat{v}\|_{1,\hat{S}_i},$$

where we used the norm equivalence on finite dimensional vector spaces and hence the constant C depends only on the radius of B_0 and B_1 but not on the shape of $\hat{S}_i$. Since $\hat{Q}_i$ maps any constant function a to itself, one has

$$|\hat{Q}_i\hat{v}|_{1,\hat{S}_i} = \inf_{a \in \mathbb{R}} |\hat{Q}_i(\hat{v} - a)|_{1,\hat{S}_i} \le C \inf_{a \in \mathbb{R}} \|\hat{v} - a\|_{1,\hat{S}_i} \le C|\hat{v}|_{1,\hat{S}_i},$$

where in the last step we have used the Bramble-Hilbert lemma (2.6) on $\hat{S}_i$.

Noticing that under the uniform scaling one has $|Q_i v|_{1,S_i} = |\hat{Q}_i \hat{V}|_{1,\hat{S}_i}$ and $|v|_{1,S_i} = |\hat{V}|_{1,\hat{S}_i}$, this completes the proof of the lemma. □

In the rest of the paper, we shall always assume that the mesh contains convex polygons and satisfies assumptions $(H1) - (H6)$. Next we can prove the main estimates of the Clément interpolations Π and Π_0.

Theorem 2.1. *For each $T \in \mathcal{T}_h$, one has*

$$|v - \Pi v|_{k,T} \leq Ch^{q-k}|v|_{q,S_T}, \text{for } k = 0,1, \; q = 1,2 \text{ and } v \in H^q(\Omega) ,$$

where C is a positive constant independent of T, h or v, and

$$S_T = \bigcup_{v_i \in \overline{T}} S_i.$$

Proof. Without loss of generality, denote by v_i, $1 \leq i \leq n$ the vertices of T. Then by (2.1) one has

$$\begin{aligned} |v - \Pi v|_{k,T} &= \left| v - \sum_{i=1}^{n} Q_i v(\boldsymbol{v}_i)\varphi_i \right|_{k,T} \\ &\leq \left| v - \sum_{i=1}^{n} Q_1 v(\boldsymbol{v}_i)\varphi_i \right|_{k,T} + \left| \sum_{i=2}^{n} (Q_1 v - Q_i v)(\boldsymbol{v}_i)\varphi_i \right|_{k,T} \\ &= |v - Q_1 v|_{k,T} + \left| \sum_{i=2}^{n} (Q_1 v - Q_i v)(\boldsymbol{v}_i)\varphi_i \right|_{k,T} \\ &\leq |v - Q_1 v|_{k,S_1} + \left| \sum_{i=2}^{n} (Q_1 v - Q_i v)(\boldsymbol{v}_i)\varphi_i \right|_{k,T}. \end{aligned} \tag{2.7}$$

We first estimate the term $|v - Q_1 v|_{k,S_1}$. For $k = 0$, by the Bramble-Hilbert lemma one has

$$\|v - Q_1 v\|_{S_1} = \inf_{\chi \in P_1(S_1)} \|v - \chi\| s_1 \leq ch^q |v|_{q,S_1}.$$

For $k = 1$, again by the Bramble-Hilbert lemma we know that for each v there exists a $\chi \in P_i(S_i)$ such that $|v - \chi|_{1,S_1} \leq Ch^{q-1}|v|_{q,S_1}$. Then, by Lemma 2.2 and the fact that $Q_1\chi = \chi$ one gets

$$|v - Q_1 v|_{1,S_1} \leq |v - \chi|_{1,S_1} + |Q_1(v - \chi)|_{1,S_1} \leq C|v - \chi|_{1,S_1} \leq Ch^{q-1}|v|_{q,S_1}.$$

Combining the above, one has

$$|v - Q_1 v|_{k,S_1} \leq Ch^{q-k}|v|_{q,S_1} \leq Ch^{q-k}|v|_{q,S_T}.$$

Then we consider the second term in the right-hand side of Inequality (2.7). Since the values of all λ_i lie in [0,1] and $\nabla\lambda_i$ are bounded as in Lemma 2.1, by the regularity assumption of the mesh, it is clear that

$$|\varphi_i|_{k,T} \leq Ch^{1-k} \text{ for } k = 0,1. \tag{2.8}$$

Denote by v_T the center of the largest disk in T, and K_i the triangle formed by vertices v_T, v_i and v_{i+1}. By the regularity assumption of the mesh, obviously each K_i is also a regular triangle, i.e, all three edges of K_i have

length of $O(h)$ and the largest internal angle of K_i is bounded away from π. Note that $Q_1 v - Q_i v$ is alinear polynomial. By the scaling argument on K_i, one has

$$\begin{aligned}|(Q_1 v - Q_i v)(v_i)| &\le Ch^{-1}\|Q_1 v - Q_i v\|_{0,K_i} \\ &\le Ch^{-1}(\|v - Q_1 v\|_{0,K_i} + \|v - Q_i v\|_{0,K_i}) \\ &\le Ch^{-1}(\|v - Q_1 v\|_{0,S_1} + \|v - Q_i v\|_{0,S_i}) \\ &\le Ch^{q-1}(|v|_{q,S_1} + |v|_{q,S_i}) \\ &\le Ch^{q-1}|v|_{q,S_T}.\end{aligned}$$

Therefore

$$|\sum_{i=2}^{n}(Q_1 v - Q_i v)(v_i)\varphi_i|_{k,T} \le C\sum_{i=2}^{n} h^{q-k}\,|v|_{q,S_T} = C(n-1)h^{q-k}|v|_{q,S_T}.$$

Combining the above and using assumption (H3), we have

$$|v - \Pi v|_{k,T} \le Ch^{q-k}|v|_{q,S_1} + C(n-1)h^{q-k}|v|_{q,S_T} \le Ch^{q-k}|v|_{q,S_T}.$$

This completes the proof of the theorem. □

Corollary 2.1. *For* $k = 0,1$ *and* $q = 1,2$, *the Clément interpolation* Π *satisfies*

$$|v - \Pi v|_k \le Ch^{q-k}|v|_q, \textit{for all } v \in H^q(\Omega)\ . \tag{2.9}$$

In particular it has the following H^1 *stability*:

$$|\Pi v|_1 \le C|v|_1, for\ all\ v \in H^q(\Omega)\ . \tag{2.10}$$

Proof. Equation (2.9) follows directly from Theorem 2.7 and conditions (H3), (H5). Equation (2.10) follows from (2.9) with $k = q = 1$ and a triangle inequality. □

Theorem 2.2. *For* $k = 0,1$ *and* $q = 1,2$, *the Clément interpolation* Π_0 *satisfies* $|v - \Pi_0 v|_k \le Ch^{q-k}|v|_q$, *for all* $v \in H_0^1(\Omega) \cap H^q(\Omega)$.

In particular it has the following H^1 *stability*:

$$|\Pi_0 v|_1 \le C|v|_1, \textit{for all } v \in H_0^1\ () \cap H^q(\Omega)\ .$$

Proof. By Corollary 2.1 and the triangle inequality, We only need to prove

$$|(\Pi - \Pi_0)v|_k \le Ch^{q-k}|v|_q.$$

Noticing that Πv and $\Pi_0 v$ are identical on internal polygons, thus it reduces to proving

$$|(\Pi - \Pi_0)v|_{k,T} \le Ch^{q-k}|v|_{q,S_T},$$

for all $T \in \mathcal{T}_h$ satisfying $\partial T \cap \partial\Omega \neq \emptyset$. Without loss of generality, assume the first m vertices of T lie on $\partial\Omega$. Then by (2.8) one has

$$|(\Pi - \Pi_0)v|_{k,T} = |\sum_{i=1}^{m} Q_i\, v(v_i)\varphi_i|_{k,T} \le \sum_{i=1}^{m} |\,Q_i v(v_i)||\varphi_i|_{k,T} \le Ch^{1-k}\sum_{i=1}^{m} |\,Q_i v(v_i)|.$$

For each v_i, $i = 1, ..., m$, there exists an edge $\gamma_i \subset \partial T \cap \partial\Omega$ such that v_i is an end of the edge γ_i. By assumption (H2), the length of γ_i is of $O(h)$. Using the scaling argument on γ_i, the fact that $v = 0$ on $\partial\Omega$ and the trace inequality (2.4), one gets

$$\begin{aligned} |Q_i v(v_i)| &\le Ch^{-1/2}\|Q_i v\|_{0,\gamma_i} = Ch^{-1/2}\|v - Q_i v\|_{0,\gamma_i} \\ &\le C(h^{-1}\|v - Q_i v\|_T + |v - Q_i|_{1,T}) \\ &\le Ch^{q-1}|v|_{q,S_i}. \end{aligned}$$

Combining the above, this completes the proof of the theorem. □

3 Finite Element Approximation

In this section we construct a polygonal finite element discretization for the Stokes equations using the generalized barycentric coordinates. The element is an extension of the Bernardi-Raugel (BR) element [1] as it is degenerates to the BR element on triangles.

Let $U = (H_0^1(\Omega))^2$ and $V = L_0^2$ The variational form of Problem (1.1) can be written as: *Find* $u \in U$ *and* $p \in V$ *such that*

$$\begin{cases} a(u,v) + b(v,p) = (f,v) & for\ all\ v \in U, \\ b(u,q) = 0 & for\ all\ q \in V, \end{cases} \tag{3.1}$$

where

$a(u,v) = (\nabla u, \nabla v)$ and $b(v,q) = -(div\ \ v, q)$.

It is well-known that Problem (3.1) admits a unique solution. Given finite dimensional sub- spaces $U_h \subset U$ and $V_h \subset V$, one can define the finite element discretization to Problem (3.1) as: *Find* $u_h \in U_h$ *and* $p_h \in V_h$ *such that*

$$\begin{cases} a(u_h,v) + b(v,p_h) = (f,v) & for\ all\ v \in U_h, \\ b(u_h,q) = 0 & for\ all\ q \in V_h. \end{cases} \tag{3.2}$$

3.1 Finite element spaces

We first define the finite element spaces U_h and V_h. Consider an element $T \in \mathcal{T}_h$ with n vertices. Define on T a set of vector-valued functions

$$w_i = n_i\lambda_i\lambda_{i+1} \text{ for } i = 1,2, \dots n,$$

where $\{\lambda_i\}_{i=1}^n$ is a set of GBCs defined on T and n_i is the unit outward normal vector on the ith edge e_i of T. Note that w_i vanishes on $\partial\Omega\backslash e_i$. Then, we introduce the local finite element space for the velocity on T as follows:

$$U_T = \Lambda_T^2 \oplus span\{w_i, i = 1,2,n\}.$$

It is clear that $\dim(U_T) = 3n$. Define the degrees of freedom for U_T by

$$\begin{cases} the\ first\ component\ of\ w(v_i)\ for\ i = 1, \dots, n, \\ the\ second\ component\ of\ w(v_i) for\ i = 1, \dots, n, \\ \frac{1}{|e_i|}\int_{e_i} w \cdot n_i ds\ for\ i = 1, \dots, n, \end{cases} \tag{3.3}$$

where $|e_i|$ is the length of edge e_i and w is a vector-valued function on T.

Lemma 3.1. *A function* w *in* U_T *can be uniquely determined by the degrees off reedom given in* (*3.3*). *In addition, on an edge* e_i, *the value of* w *depends only on the degrees offreedom associated with* e_i, *i.e.*, $w(v_i)$, $w(v)$ *and* $\frac{1}{|e_i|}\int_{e_i} w \cdot n_i ds$.

Proof. For the unisolvency, it is sufficient to prove that when all degrees of freedom in (3.3) vanish, then $w \equiv 0$. Consider

$$w = \sum_{i=1}^{n} \alpha_i w_i + \sum_{i=1}^{n} \beta_i \begin{bmatrix} \lambda_i \\ 0 \end{bmatrix} + \sum_{i=1}^{n} \gamma_i \begin{bmatrix} 0 \\ \lambda_i \end{bmatrix} \in U_T.$$

Since w_i vanishes on all vertices of T, it is clear that $w(v_i) = 0$ for all i immediately implies that $\beta_i = \gamma_i = 0$, for $i = 1, ..., n$. We are left with $w = \sum_{i=1}^{n} \alpha_i w_i$. Since w_i vanishes on all edges except for e_i, one has

$$0 = \int_{e_i} w \cdot n_i ds = \int_{e_i} \alpha_i w_i \cdot n_i ds = \alpha_i \int_{e_i} \lambda_i \lambda_{i+1} ds,$$

which further implies that $\alpha_i = 0$ for $i = 1, ..., n$. Therefore $w \equiv 0$.

Likewise, when $w(v_i) = w(v_{i+1}) = 0$ and $\int_{e_i} \alpha_i w_i \cdot n_i ds = 0$, we can easily deduce that $w|_{e_i} \equiv 0$. This completes the proof of the lemma. □

Lemma 3.1 guarantees that the local finite element spaces U_T can be glued together into an H^1 conforming global finite element space:

$$U_h = \{ v \in U \text{ such that } v|\tau \in U_T \text{ for } T \in \mathcal{T}_h \}.$$

The space U_h can be viewed as $\Lambda_{0,h}^2$ plus edge bubbles, one for each interior edge. Thus

$$\dim U_h = 2 * (\text{ \# of interior vertices in } \mathcal{T}_h) + (\text{ \# of interior edges in } \mathcal{T}_h)$$

We shall use U_h to discretize the velocity. The pressure will be discretized using the space of piecewise constants, that is,

$$V_h = \{ q \in V \text{ such that } q|\tau \in P_0(T) \text{ for } T \in \mathcal{T}_h \}.$$

3.2 The discrete inf-sup condition

Following the standard mixed finite element analysis [4,3], one obtains the well-posedness and the approximation property of Equation (3.2) if the dis- crete spaces U_h and V_h satisfy the inf-sup condition

$$\sup_{\boldsymbol{v} \in \boldsymbol{U}_h} \frac{b(\boldsymbol{v}, p)}{\|\boldsymbol{v}\|_1} \geq C\|p\| \qquad \text{for all } p \in V_h. \tag{3.4}$$

In this section, we prove (3.4) by constructing a Fortin operator from U to U_h.

With a little abuse of the notation, we extend the Clément interpolation $\Pi_0 : H_0^1(\Omega) \to \Lambda_{0,h}$ to the product spaces $\Pi_0 : U \to \Lambda_{0,h}^2$. Then, we define a Fortin operator $\pi_h : U \to U_h$ by:

$$\begin{cases} \pi_h u(v) = \Pi_0 u_0(v) & for\ each\ vertex\ v\ of\ \mathcal{T}_h \\ \int_e (\pi_h u - u) \cdot n ds & for\ each\ edge\ e\ of\ \mathcal{T}_h \end{cases} \tag{3.5}$$

By Lemma 3.1, it is easy to see that π_h is well-defined. Moreover, we ha

Theorem 3.1. *The operator π_h satisfies*

(*commutativity*) $b(\pi_h u - u, q_h) = 0$ *for all* $u \in U$ *and* $q_h \in V_h$,
(*stability*) $|\pi_h u|_1 \leq C|u|_1$ *for all* $u \in U$,
(*approximability*) $|u - \pi_h u|_1 \leq Ch|u|_2$ *for all* $u \in U \cap (H^2(\Omega))^2$

Proof. By the Green's formula and the definition of π_h, one has

$$\begin{aligned} b(\pi_h u - u, q_h) &= -\int_\Omega q_h \,\mathrm{div}(\pi_h u - u)dx \\ &= -\sum_{T\in\mathcal{T}_h} q_h \int_T \mathrm{d\,iv}(\pi_h u - u)dx \\ &= -\sum_{T\in\mathcal{T}_h} q_h \int_{\partial T} (\pi_h u - u)\cdot n ds \\ &= 0. \end{aligned}$$

This completes the proof of the commutativity for the Fortin operator.

Next, to prove the stability of the Fortin operator, it suffices to prove that

$$|\pi_h u - u|_{1,T} \leq C|u|_{1,S_T}.$$

For $T \in \mathcal{T}_h$, from the definition of the Fortin operator it is clear that

$$\pi_h u - \Pi_0 u = \sum_{i=1}^{n} \alpha_i w_i,$$

with

$$\alpha_i = \frac{\int_{e_i}(u - \Pi_0 u)\cdot n_i ds}{\int_{e_i} w_i \cdot n_i ds} = \frac{\int_{e_i}(u - \Pi_0 u)\cdot n_i ds}{\int_{e_i} \lambda_i \lambda_{i+1} ds} = \frac{6}{|e_i|}\int_{e_i}(u - \Pi_0 u)\cdot n_i ds.$$

By the Schwarz inequality, Assumption (H2), the trace inequality (2.4) and Theorem 2.2, one immediately gets

$$\begin{aligned} |\alpha_i| &\leq \frac{6}{|e_i|}(|e_i|^{\frac{1}{2}}\|u - \Pi_0 u\|_{0,e_i}) \leq Ch^{-\frac{1}{2}}\|u - \Pi_0 u\|_{0,e_i} \\ &\leq C(h^{-1}\|u - \Pi_0 u\|_{0,T} + |u - \Pi_0 u|_{1,T}) \quad (3.6) \\ &\leq C|u|_{1,S_T}. \end{aligned}$$

Using the triangle inequality, one has

$$|\pi_h u - u|_{1,T} = |\Pi_0 u - u + \textstyle\sum_{i=1}^{n} \alpha_i w_i|_{1,T} \tag{3.7}$$

$$\leq |\Pi_0 u - u|_{1,T} + |\sum_{i=1}^{n} \alpha_i w_i|_{1,T}$$

By Theorem 2.2, the first term in the right-hand side of (3.7) satisfies

$$|\Pi_0 u - u|_{1,T} \leq C|u|_{1,S_T} \tag{3.8}$$

For the second term, note that by $\lambda_i \leq 1$ on T and Lemma 2.1,

$$\begin{aligned} |w_i|_{1,T} &= |n_i\lambda_i\lambda_{i+1}|_{1,T} \leq C\|\nabla(\lambda_i\lambda_{i+1})\|_{0,T} \\ &= C\|\lambda_i\nabla\lambda_{i+1} + \lambda_{i+1}\nabla\lambda_i\|_{0,T} \\ &\leq C(\|\nabla\lambda_{i+1}\|_{0,\tau+}\|\nabla\lambda_i\|_{0,T}) \\ &\leq C|T|^{\frac{1}{2}}h^{-1} \leq C. \end{aligned} \tag{3.9}$$

Combining the above gives $|\pi_h u - u|_{1,T} \leq C|u|_{1,S_T}$. This together with assumptions (H3) and (H5) completes the proof of the stability for π_h.

Finally, we prove the approximability. Note that when $u \in U \cap (H^2(\Omega))^2$ inequalities (3.6) and (3.8) can be improved into

$$|\alpha_i| \leq Ch|u|_{2,S_T}, |\Pi_0 u - u|_{1,T} \leq Ch|u|_{2,S_T}.$$

These, combined with assumptions (H3), (H5) and inequalities (3.7), (3.9), give the desired ap- proximability estimate. □

Since the Fortin operator π_h is commutative and stable, it is standard [4, 3] to show that

Corollary 3.1. *The finite element spaces U_h and V_h satisfy the inf-sup condition* (3.4). *Conse- quently the discrete problem* (3.2) *admits a unique solution*.

3.3 Error estimates

In this sub-section, we derive the error estimates for the discrete problem (3.2). Since the finite element spaces U_h and V_h satisfy the discrete inf-sup condition (3.4), by the standard mixed finite element theory [4, 3] one has

$$\|\boldsymbol{u} - \boldsymbol{u}_h\|_1 + \|p - p_h\| \leq C\left(\inf_{\boldsymbol{\psi}\in\boldsymbol{U}_h}\|\boldsymbol{u} - \boldsymbol{\psi}\|_1 + \inf_{q\in V_h}\|p - q\|\right) \tag{3.10}$$

where u and p are solutions to the variational problem (3.1) and u_h and p_h are solutions to the discrete problem (3.2).

Using the approximability of the Fortin operator, one has

$$\inf_{\boldsymbol{\psi}\in\boldsymbol{U}_h}\|\boldsymbol{u} - \boldsymbol{\psi}\|_1 \leq \|u - \pi u\|_1 \leq Ch|\boldsymbol{u}|_2.$$

Using (2.3), we get

$$\inf_{q\in V_h}\|p - q\| \leq Ch|p|_1.$$

Combining the above, this gives the optimal error estimate in the energy norm:

Theorem 3.2. *Let (u, p) and (u_h, p_h) be the solutions to* (*3.1*) *and* (*3.2*) *respectively then*

$$\|u - u_h\|_1 + \|p - p_h\|_0 \leq Ch(|u|_2 + |p|_1)\ . \tag{3.11}$$

Next, we derive an L^2 error estimate for the velocity. To this end, we first introduce a dual problem

$$\begin{cases} -\Delta\chi + \nabla\eta = u - u_h & \text{in } \Omega, \\ \text{div}\chi = 0 & \text{in}\Omega, \\ \chi = 0 & \text{on } \partial\Omega, \end{cases} \tag{3.12}$$

When Ω is convex, the dual problem has full regularity [3], i.e., $\chi \in (H_0^1(\Omega) \cap H^2(\Omega))^2$ and $\eta \in L_0^2(\Omega) \cap H^1$ () satisfy

$$\|\chi\|_2 + \|\eta\|_1 \leq C\|u - u_h\|. \tag{3.13}$$

Theorem 3.3. *When the dual problem has full regularity* (3.13), *one has*

$$\|u - u_h\| \leq Ch^2(|u|_2 + |p|_1) .$$

Proof. The proof is standard. By subtracting (3.2) from (3.1) one gets

$$\begin{cases} (\nabla(u - u_h), \nabla v) - (\text{div } v, p - p_h) = 0 & \text{for all v} \in \text{U}_\text{h} \\ (\text{div}(u - u_h), q) = 0 & \text{for all q} \in \text{V}_\text{h}. \end{cases}$$

Denote by $Q_h : V \to V_h$ the L^2 orthogonal projection. Then we have

$$\begin{aligned} \|u - u_h\|^2 &= (u - u_h, -\Delta\chi + \nabla\eta) \\ &= (\nabla(u - u_h), \nabla\chi) - (\text{div}(u - u_h), \eta) \\ &= (\nabla(u - u_h), \nabla(\chi - \pi\chi)) + (\text{div}(\pi\chi), p - p_h) - (\text{div}(u - u_h), \eta - Q_h\eta) \\ &= (\nabla(u - u_h), \nabla(\chi - \pi\chi)) + (\text{div}(\chi - \pi\chi), p - p_h) - (\text{div}(u - u_h), \eta - Q_h\eta) . \end{aligned}$$

Using the Schwarz inequality, Theorem 3.2, the Bramble-Hilbert lemma (2.3) and the regularity (3.13), we get

$$\|u - u_h\|^2 \leq Ch^2(|u|_2 + |p|_1)(|\chi|_2 + |\eta|_1) \leq Ch^2(|u|_2 + |p|_1)\|u - u_h\|.$$

This completes the proof of the lemma. □

4 Numerical Example

In this section, we test the performance of extended BR element using the following example problem:

Example. Set $\Omega = (0,1) \times (0,1)$ and the exact solution

$$u = a_u \begin{pmatrix} sin(2\pi x)cos(2\pi y) \\ -cos(2\pi x)sin(2\pi y) \end{pmatrix}, p = a_p(\sin(\pi x)\sin(\pi y) - \tfrac{4}{\pi^2}) ,$$

where $a_u, a_p \in \mathbb{R}$ are parameters that can be adjusted later. For now we simply set $a_u = a_p = 1$. Note that the pressure is mean-value free.

In all numerical experiments, we use the Wachspress coordinates to build the extended BR element. The results are compared with numerical results from the extended PIPO/QIPO element [16] built again with the Wachspress coordinates. For simplicity, in the rest of this section we shall address the extended PIPO/QIPO element by $PlP0$ element" and the extended BR element by "BR element". Note that the only difference between the construction of the BR element and the PIPO element is the presence of edge bubbles. We have proved that the BR element is stable on polygonal meshes, while the PIPO element is in general not.

We compare the convergence rates of the BR and the PIPO elements on four types of meshes as shown in Fig. 1: uniform rectangular, pentagonal, hexagonal meshes and the centroidal Voronoi tessellations (CVTs) [29]. The CVT is a type of Voronoi tessellation where the generator of each polygon is identical to the barycenter of the polygon. Each internal vertex of a CVT mesh is connected to at most three edges. We point out that this is also true for the hexagonal mesh in Fig. 1. Thus according to [16], the PIPO element is stable on the hexagonal and CVT meshes. It is known that the PIPO element is not stable on uniform rectangular meshes. Although it does

give optimal approximation for the velocity, but the pressure admits a check-board type spurious mode [6, 7]. The remaining one is the pentagonal mesh, on which we do not have any theoretical knowledge about the stability of the PIPO element.

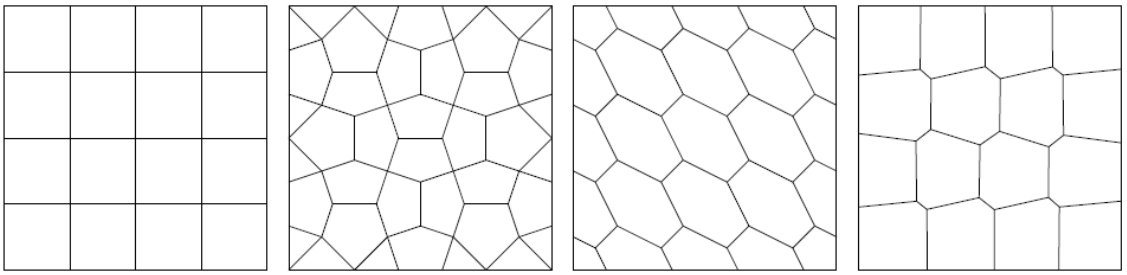

Fig. 1. Different meshes with approximate size $h = 0.25$. From left to right: (1) a uniform rectangular mesh; (2) a uniform mesh consisting of mostly pen- tagons; (3) a uniform mesh consisting of mostly hexagons; (4) a CVT mesh

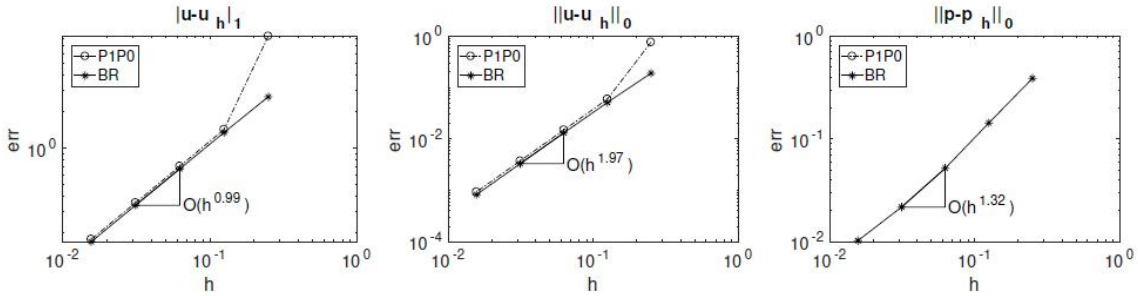

Fig. 2. Convergence rates on the rectangular mesh

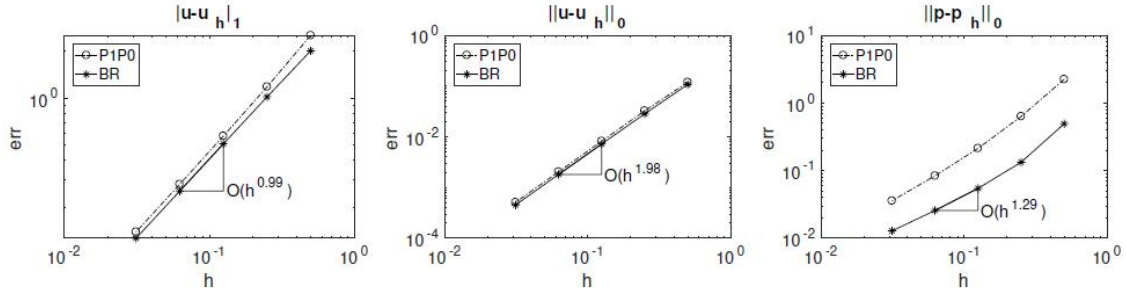

Fig. 3. Convergence rates on the mostly pentagonal mesh

We run the test for $h = \frac{1}{4}, \frac{1}{8}, \frac{1}{16}, \frac{1}{32}, \frac{1}{64}$, and report the errors for both the velocity and the pressure in Figs. 2-5. From the figures we see that the BR element and the PIPO element behaves almost the same on pentagonal and CVT meshes, on which the PIPO element is known to be stable. On uniform rectangular meshes, the pressure computed using the PIPO element is polluted by the check-board spurious mode and hence its convergence rate is not calculated. The most interesting part happens on pentagonal meshes, on which the BR and the PIPO elements give significantly different error for the pressure, as shown in Fig. 3. We also emphasize that since the BR element is stable on arbitrary convex polygonal meshes, in all numerical tests it gives optimal convergence for both the velocity and the pressure. The convergence rate of the pressure appears to be greater than the known optimal rate $O(h)$ for piecewise constants, which is another interesting issue and will be investigated later.

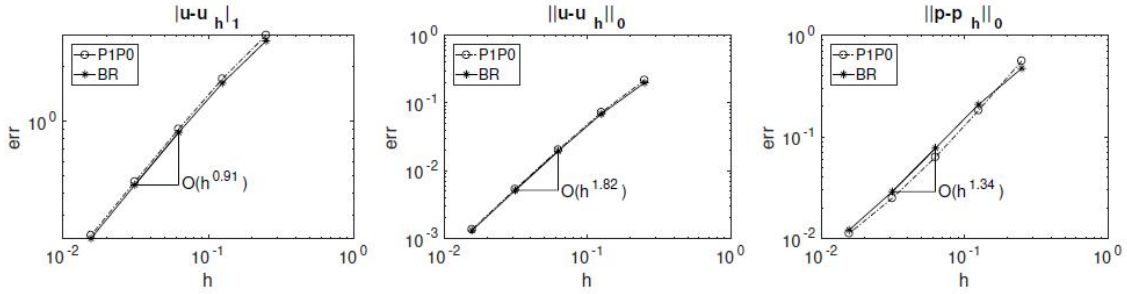

Fig. 4. Convergence rates on the mostly hexagonal mesh

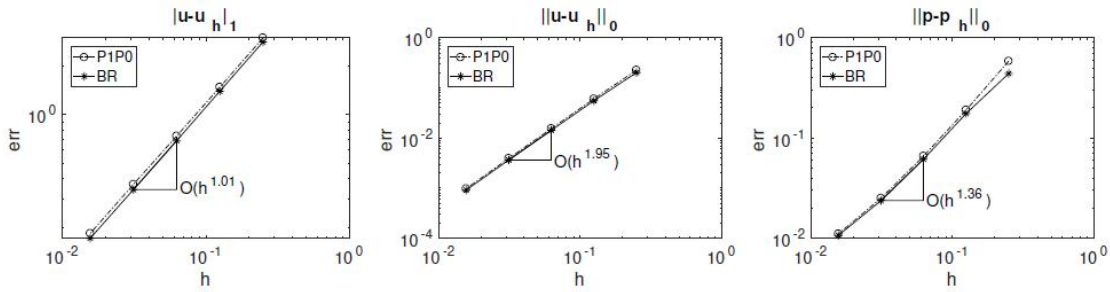

Fig. 5. Convergence rates on the CVT mesh

To further examine the difference between the BR and the PIPO elements on pentagonal meshes, we solve the test problem with $a_p = 0$. This sets the exact pressure $p \equiv 0$ while the exact velocity remains unchanged. Without the interference of the physical pressure, the graph of the numerical pressure will clearly reveal spurious modes, if there is any. We draw the numerical pressure, computed using the BR element and the PIPO element, respectively, in Fig. 6. From the graph, it is clear that the numerical pressure of the PIPO element exhibits strong oscillations especially near $\partial\Omega$, while the numerical pressure from the stable BR element behaves much better.

Finally, we explore the seemingly unreasonable fact that the convergence rates of the pressure in Figs, 2-5 all exceed $O(h)$, the optimal rate that can be achieved by piecewise constant approx- imations. Similar phenomena have been observed before in [16, 20, 18]. In our implementation, $\|p - p_h\|$ is computed using high order Gaussian quadratures on the sub-triangulation of mesh elements. Therefore, this is not a super-convergence caused by using low-order numerical integra- tion. Recall it is generally known that if the exact solution has $p = 0$, some finite elements for the Stokes equations can achieve better convergence rates. For example, the $P2P0$ element has only first-order overall convergence but it behaves like a second order element if the exact pressure is 0. Based on this knowledge, we examine the convergence rate of the BR element on CVT meshes under the following settings:

(1) $a_u = 1, a_p = 0$, which means the exact solution has $p \equiv 0$;
(2) $a_u = a_p = 1$;
(3) $a_u = 0, a_p = 1$, which means the exact solution has $u \equiv 0$.

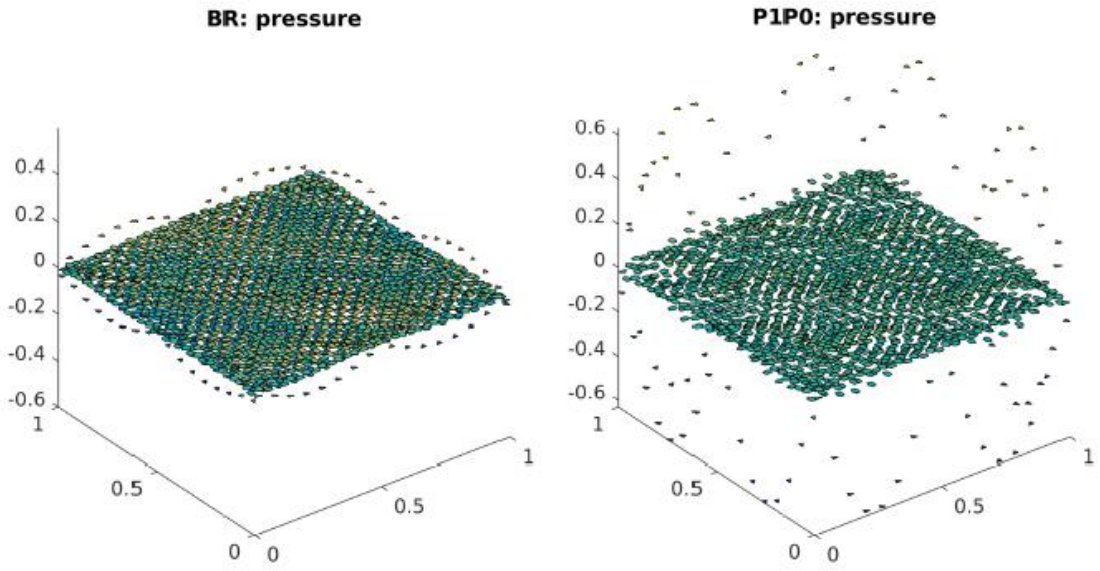

Fig. 6. Spurious modes in the numerical pressure

The results are reported in Fig. 7. Note that both $|u-u_h|_1$ and $\|u-u_h\|_0$ still have the same optimal convergence rates, while the actual error becomes much smaller when the exact solution has $u \equiv 0$. This is understandable. It is interesting that the convergence rates for $\|p-p_h\|_0$ seem to vary from $o(h^{1:02})$ for the $u \equiv 0$ case to $o(h^{1:67})$ for the $p \equiv 0$ case. We point out that the $o(h)$ convergence rate, i.e., the worst-case scenario, is around the optimal convergence rate guaranteed by the theory. It occurs when p is dominant. As the exact pressure decreases to *0*, the convergence rate of $\|p-p_h\|_0$ increases. Our conjecture is that an improved error estimate can possibly be proved for the extreme case when $p \equiv 0$. This makes a good topic for future research.

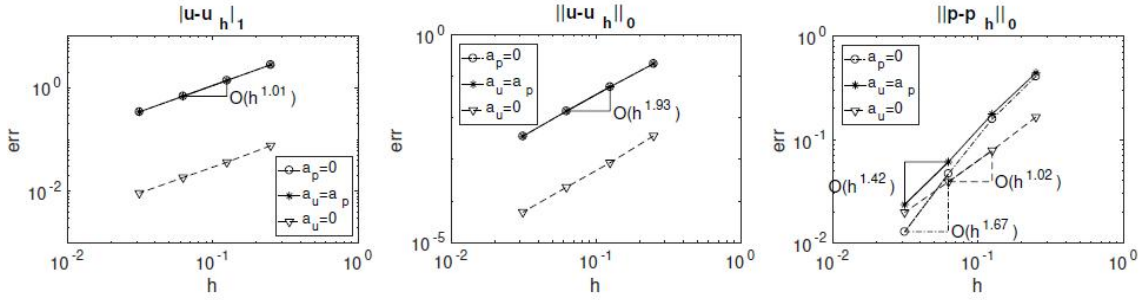

Fig. 7. Convergence rates on the CVT mesh, with different values for a_u and a_p..

5 Conclusion

In this paper, the mixed finite element method for Stokes equations on polygonal meshes is discussed in detail. By using the generalized barycenter coordinates, the Bernardi-raugel element on triangular meshes is extended to polygonal meshes. It is proved theoretically and numerically that the method is stable, that is, it satisfies the discrete LBB condition.

At present, we regard the finite element on polygonal mesh as an extension from triangular element and rectangular element to general convex polygon, which is not only a good supplement to the existing methods, In the future, we will consider how to construct Higher-Order Finite Elements on polygonal meshes and how to extend other finite elements on traditional triangular meshes to polygonal meshes

Competing Interests

Author has declared that no competing interests exist.

References

[1] Bernardi C, Raugel G. Analysis of some finite elements for the Stokes problem, Math. Comp. 1985;44: 71-79.

[2] Brenner S, Scott L. The mathematical theory offinite element methods, Springer, New York; 2007.

[3] Girault V, Raviart P. Finite element methods for Navier-Stokes equations, Springer, Berlin; 1986.

[4] Boffi D, Brezzi F, Fortin M. Mixed finite element methods and applications, Springer, New York; 2013.

[5] Pitkäranta J, Stenberg R. Analysis of some mixedfinite element methods for plane elasticity equations, Math. Comp. 1983;41:399-423.

[6] Sani R, Gresho P, Lee R, Griffiths D. The cause and cure (?) of the spurious pressures generated by certain FEM solutions of the incompressible Navier-Stokes equations: Part 1, Int. J. Numer. Methods Fluids. 1981;1:17-43.

[7] Sani R, Gresho P, Lee R, Griffiths D, Engelman M. The cause and cure (!) of the spurious pressures generated by certain FEM solutions of the incompressible Navier-Stokes equations: Part 2, Int. J. Numer. Methods Fluids. 1981;1:171-204.

[8] Floater M. Wachspress and mean value coordinates, in Approximation Theory XIV: San Antonio, Springer. 2013;81-102.

[9] Floater M. Generalized barycentric coordinates and applications, Acta Numerica. 2015;161-214.

[10] Floater M, Hormann K, KÓs G. A general construction of barycentric coordinates over convex poly- gons, Adv. Comput. Math. 2006;24:311-331.

[11] Wachspress E. A rational finite element basis, Academic Press; 1975.

[12] Warren J, Schaefer S, Hirani A, Desbrun M. Barycentric coordinates for convex sets, Adv. Comput. Math., 2007;27:319-338.

[13] Bishop J. A displacement-based finite element formulation for general polyhedra using harmonic shape functions. Int. J. Numer. Meth. Engng. 2014;97:1-31.

[14] Manzini G, Russo A, Sukumar N. New perspectives on polygonal and polyhedral finite element methods, Math. Models Methods Appl. Sci. 2014;24:1665-1699.

[15] Sukumar N, Tabarraei A. Conforming polygonal finite elements, Int. J. Numer. Meth. Engng. 2004;61: 2045-2066.

[16] Talischi C, Pereira A, Paulino G, Menezes I, Carvalho M. Polygonal finite elements for incompressible fluid flow, Int. J. Numer. Meth. Fluids. 2014;74:134-151.

[17] Beirão da Veiga L, Lipnikov K. A mimetic discretization of the Stokes problem with selected edge bubbles, SIAM J. Sci. Comp. 2010;32:875-893.

[18] Vu-Huu T, Le-Thanh C, H. Nguyen-Xuan AND M. Abdel-Wahab, An equal-order mixed polygonal finite elementfor two-dimensional incompressible Stokes flows, Euro. J. Mech. /B Fluids. 2020;79:92-108.

[19] Dohrmann C, Bochev P. A stabilized finite element method for the Stokes problem based on polynomial pressure projections, Int. J. Numer. Methods Fluids. 2004;46:183-201.

[20] Vu-Huu T, Le‐Thanh C, Nguyen-Xuan H, Abdel-Wahab M. A high-ordermixedpolygonalfinite element for incompressible Stokes flow analysis, Comput. Methods Appl. Mech. Engrg. 2019;356:175-198.

[21] Clément P. Approximation by finite elementfunctions using local regularization, RAIRO Anal. Numer., R-2. 1975;77-84.

[22] Meyer M, Barr A, Lee H, Desbrun M. Generalized barycentric coordinates on irregular polygons, J. Graph. Tools. 2002;7:13-22.

[23] Mu L, Wang X, Wang Y. Shape regularity conditions for polygonallpolyhedral meshes, exemplified in a discontinuous Galerkin discretization, Numer. Meth. Part. Diff. Eqs. 2015;31:308-325.

[24] Floater M, Gillette A, Sukumar N. Gradient bounds for Wachspress coordinates on polytopes, SIAM J. Numer. Anal. 2014;52:515-532.

[25] Gillette A, Rand A, Bajaj C. Error estimatesfor generalized barycentric interpolation, Adv. Comput. Math., 2012;37:417-439.

[26] Rand A, Gillette A, Bajaj C. Interpolation error estimates for mean value coordinates over convex polygons, Adv. Comput. Math. 2013;39:327-347.

[27] Scott L, Zhang S. Finite element interpolation of nonsmooth functions satisfying boundary condition, Math. Comp. 1990;54:483-493.

[28] Bramble J, Xu J. Some estimates for a weighted L^2 projection, Math. Comp. 1991;56:463-476.

[29] Du Q, Faber V, Gunzburger M. Centroidal Voronoi tessellations: Applications and algorithms, SIAM Rev., 1999;41:637-676.

Peer-review history:
The peer review history for this paper can be accessed here (Please copy paste the total link in your browser address bar)
http://www.sdiarticle4.com/review-history/68717